Computers and Mathematics with Applications 59 (2010) 215–224

Contents lists available at ScienceDirect

Computers and Mathematics with Applications

journal homepage: www.elsevier.com/locate/camwa

A nonlinear weighted least-squares finite element method for Stokes equations

Hsueh-Chen Lee [a], Tsu-Fen Chen [b,*]

[a] General Education Center, Wenzao Ursuline College of Languages, Kaohsiung, Taiwan

[b] Department of Mathematics, National Chung Cheng University, Minghsiung, Chia-Yi, Taiwan

ARTICLE INFO

Article history:
Received 22 July 2009
Accepted 5 August 2009

Keywords:
Least-squares finite element methods
Stokes problems
Nonlinear weighted function
Mass conservation

ABSTRACT

The paper concerns a nonlinear weighted least-squares finite element method for the solutions of the incompressible Stokes equations based on the application of the least-squares minimization principle to an equivalent first order velocity–pressure–stress system. Model problem considered is the flow in a planar channel. The least-squares functional involves the L^2-norms of the residuals of each equation multiplied by a nonlinear weighting function and mesh dependent weights. Using linear approximations for all variables, by properly adjusting the importance of the mass conservation equation and a carefully chosen nonlinear weighting function, the least-squares solutions exhibit optimal L^2-norm error convergence in all unknowns. Numerical solutions of the flow pass through a 4 to 1 contraction channel will also be considered.

1. Introduction

In recent years, there have been a lot of developments in the application of least-squares methods for the approximation of the flow equations; see, e.g., [1–6]. The least-squares finite element approach for Stokes problem has been shown to offer several theoretical and computational advantages over Galerkin methods for a variety of boundary value problems [1]. In addition, the algebraic system generated by the discretization is always symmetric and positive definite, there is no compatibility condition between finite element spaces for mixed methods, and the method is insensitive to equation type. In [7], Bochev and Gunzburger introduce a weighted least-squares functional with velocity–pressure–stress formulations involving L^2-norms of the residuals of each equation multiplied by a mesh dependent weight. In addition, they extend the Agmon–Douglis–Nirenberg a priori estimate to the velocity–pressure–stress formulation of the Stokes equations. Their numerical examples indicate that the method is not optimal without the weights in the least-squares functional. In addition, if one uses the same linear approximation for all unknowns, the linear weighted least-squares method is not optimal. Similar results using H^{-1}-norm least-squares functional for Stokes equations based on the velocity–pressure–stress formulation are presented in [8]. Regardless of their advantages, poor mass conservation is reported in least-squares based formulations, see e.g., [9–11]. Note, however, as indicated in [10], results can be improved by sufficiently weighting the mass conservation term.

The purpose of the study is to present a nonlinear weighting function in the least-squares method based on the velocity–pressure–stress formulation for Stokes equations. The analysis of the nonlinear weighted least-squares functional follows the idea introduced in [7]. The choice of weights is a focus of the current effort. In this paper, we implement the nonlinear weighted least-squares formulation using linear basis functions for all variables. Using continuous piecewise linear

* Corresponding author.
E-mail addresses: 87013@mail.wtuc.edu.tw (H.-C. Lee), tfchen@math.ccu.edu.tw (T.-F. Chen).

0898-1221/$ – see front matter © 2009 Elsevier Ltd. All rights reserved.
doi:10.1016/j.camwa.2009.08.033

finite element spaces for all variables, properly adjusting the importance of the mass conservation and with carefully chosen nonlinear weighting functions, the least-squares solutions exhibit optimal L^2-norm error convergence in all dependent variables. Further, we extend the implementation to simulate the 4 to 1 contraction problem, [12]. Here we will point out that the choice of weights used to balance the residual contributions is an area that warrants further study.

Following this introduction, the stability and error estimates of a nonlinear weighted least-squares method for the Stokes equations are presented in Section 2. In Section 3, results of various least-squares finite element are provided for the flow in a planar channel and the 4 to 1 contraction problem. Conclusions are presented in Section 4.

2. Nonlinear weighted least-squares methods for Stokes equations

The section studies a nonlinear weighted least-squares method for the incompressible Stokes equations based on the velocity–pressure–stress formulation.

Consider the following generalized stationary Stokes problem in an open, boundary two-dimensional Ω with boundary Γ:

$$\begin{aligned} &-\eta\Delta\mathbf{u}+\nabla p=\mathbf{f} \quad \text{in } \Omega, \\ &\nabla\cdot\mathbf{u}=0 \quad \text{in } \Omega, \\ &\mathbf{u}=\mathbf{U} \quad \text{on } \Gamma, \end{aligned} \tag{1}$$

where $\mathbf{u}$ and p denote the velocity and pressure fields, η is a constant and $\mathbf{f}$ and $\mathbf{U}$ are given functions. We assume that the pressure p satisfies a zero mean constraint:

$$\int_\Omega p\mathrm{d}x=0.$$

Let $\mathbf{D}(\mathbf{u})=\frac{1}{2}\left(\nabla\mathbf{u}+\nabla\mathbf{u}^{\mathrm{T}}\right)$ denote the symmetric part of the velocity gradient. i.e., the deformation tensor. Defining the stress tensor $\boldsymbol{\tau}:=\sqrt{2\eta}\mathbf{D}(\mathbf{u})$ scaled by $\sqrt{\eta/2}$, we have the following generalized velocity–pressure–stress system:

$$\begin{aligned} &\boldsymbol{\tau}-\sqrt{2\eta}\mathbf{D}(\mathbf{u})=\mathbf{F}_1 \quad \text{in } \Omega, \\ &\nabla\cdot\mathbf{u}=\mathrm{f}_2 \quad \text{in } \Omega, \\ &-\sqrt{2\eta}\nabla\cdot\boldsymbol{\tau}+\nabla p=\mathbf{f}_3 \quad \text{in } \Omega, \\ &\mathbf{u}=\mathbf{u}_0 \quad \text{on } \Gamma, \end{aligned} \tag{2}$$

where the function f_2 satisfies the following solvability constraint:

$$\int_\Omega \mathrm{f}_2\mathrm{d}x=\int_{\partial\Omega}\mathbf{u}_0\cdot\mathbf{n}\mathrm{d}s.$$

Note that in two dimensions, the system (2) has six equations and six unknowns. If the tensor $\mathbf{F}_1$ and the function f_2 are identically zero, the Stokes equations (1) is equivalent to the generalized system (2). For simplicity, without loss of generality, we assume that $\mathbf{u}_0=0$.

Let $H^s(\Omega), s\geq 0$ be the Sobolev spaces with the standard inner products $(\cdot,\cdot)_s$ and their respective norms $\|\cdot\|_s$. For $s=0$, $H^s(\Omega)$ coincides with $L^2(\Omega)$. $H_0^s(\Omega)$ denotes the closure of $D(\Omega)$, the linear space of infinitely differentiable functions with compact supports on Ω, with respect to the norm $\|\cdot\|_s$. Denote by $L_0^2(\Omega)$ the subspace of square integrable functions with zero mean:

$$L_0^2(\Omega):=\left\{p\in L^2(\Omega):\int_\Omega p\mathrm{d}x=0\right\}.$$

For positive values of s, the space $H^{-s}(\Omega)$ is the dual space of $H_0^s(\Omega)$ with the norm

$$\|\phi\|_{-s}:=\sup_{0\neq v\in H_0^s(\Omega)}\frac{(\phi,v)}{\|v\|_s},$$

where $(.,.)$ is the duality pairing between $H_0^{-s}(\Omega)$ and $H_0^s(\Omega)$. Define the product spaces $\mathbf{H}_0^s(\Omega)^d=\prod_{i=1}^d H_0^s(\Omega)$ and $\mathbf{H}_0^{-s}(\Omega)^d=\prod_{i=1}^d H_0^{-s}(\Omega)$.

Let $\mathbf{H}(\mathrm{div};\Omega)=\left\{\boldsymbol{v}\in\mathbf{L}^2(\Omega)^d:\nabla\cdot\boldsymbol{v}\in L^2(\Omega)\right\}$ with the norm

$$\|\boldsymbol{v}\|_{\mathbf{H}(\mathrm{div};\Omega)}:=\left(\|\boldsymbol{v}\|_0^2+\|\nabla\cdot\boldsymbol{v}\|_0^2\right)^{\frac{1}{2}}.$$

In [7], Bochev and Gunzburger applied the Agmon–Douglis–Nirenberg (ADN) theory to establish the following a priori estimate of the first order system (2):

$$\|\boldsymbol{\tau}\|_0^2+\|p\|_0^2+\|\mathbf{u}\|_1^2\leq C\left\|\boldsymbol{\tau}-\sqrt{2\eta}\mathbf{D}(\mathbf{u})\right\|_{q+1}^2+C\|\nabla\cdot\mathbf{u}\|_{q+1}^2+C\left\|-\sqrt{2\eta}\nabla\cdot\boldsymbol{\tau}+\nabla p\right\|_q^2, \tag{3}$$

for all $q\in R$.

In the following, we describe a nonlinear weighted least-squares method associated with the system (2). Let $\boldsymbol{\Phi} := \mathbf{V} \times Q \times \boldsymbol{\Sigma} = \mathbf{H}_0^1(\Omega)^2 \times L_0^2(\Omega) \times \underline{\mathbf{L}}^2(\Omega)^3$, where $\underline{\mathbf{L}}^2(\Omega)^d$ is $d \times d$ system matrix functions whose elements are square integrable. For the finite element approximation, we assume that the domain Ω is a polygon for $d = 2$ or a polyhedron for $d = 3$ and that Γ_h is a partition of Ω into finite elements $\Omega = \bigcup_{T \in \Gamma_h} T$ with $h = \max\{\text{diam}(T) : T \in \Gamma_h\}$. Assume that the triangulation Γ_h is regular and satisfies the inverse assumption (see [8]). Let $\boldsymbol{\Phi}^h := \mathbf{V}^h \times Q^h \times \boldsymbol{\Sigma}^h$ be a finite element subspace of $\boldsymbol{\Phi}$ with the following approximation prosperities: there exists a positive integer r such that the spaces S_j approximate optimally with respect to the space $H^{r+j}(\Omega), j = 1, 2$. More precisely, we assume that for all $u \in H^{r+j}(\Omega)$ there exists an elements $u^I \in S_j$ such that $0 \le m \le 1$,

$$\left\| u - u^I \right\|_m \le Ch^{r+j-m} \|u\|_{r+j}. \tag{4}$$

The least-squares functional for (2) is defined as follows:

$$J(\mathbf{v}, q, \boldsymbol{\sigma}; \mathbf{f}) = h^{-2} \left\| w_s \left(\boldsymbol{\sigma} - \sqrt{2\eta}\mathbf{D}(\mathbf{v}) - \mathbf{F}_1 \right) \right\|_0^2 + h^{-2} K \|\nabla \cdot \mathbf{v} - \mathrm{f}_2\|_0^2 + \left\| -\sqrt{2\eta}\nabla \cdot \boldsymbol{\sigma} + \nabla q - \mathbf{f}_3 \right\|_0^2, \tag{5}$$

where K is a positive constant and is set to one here for convenience of the analysis. In the case when $w_s = 1$, Deang and Gunzburger [13] consider the positive weight K outside of the residual norm for conservation of mass in (5). They indicate that the rate of convergence can be improved by taking $K \ge 1$. In [14], a nonlinear weighted least-squares method is considered to solve nonlinear hyperbolic equations. Following [14], a nonlinear weighting function is employed in [6,15] to solve generalized Newtonian (Carreau model) flow problems. Based on the success of the nonlinear weighted least-squares approach to the generalized Newtonian flow problem, the following weighting function w_s is considered in our work. In each element, the weight w_s is taken as

$$w_s = \frac{1}{\sqrt{1 + (\dot{\gamma})^2}},$$

where the shear rate

$$\dot{\gamma} \le \dot{\gamma}_w,$$

with $\dot{\gamma} = \sqrt{2\,(\mathbf{D}(\mathbf{u}) : \mathbf{D}(\mathbf{u}))}$ and double-dot product between two second-order tensors $\boldsymbol{\tau}$ and $\boldsymbol{\sigma}$ defined as

$$\boldsymbol{\tau} : \boldsymbol{\sigma} = \sum_{i,j} \tau_{ij}\sigma_{ji}.$$

The wall shear rate $\dot{\gamma}_w$, the maximum value of the shear rate $\dot{\gamma}$, is defined as

$$\dot{\gamma}_w = \frac{\tau_w}{\eta},$$

where η is the viscosity and the wall shear stress τ_w can be directly obtained from the pressure drop and the geometric constants [16].

The least-squares problem for the first order system (2) is to minimize the quadratic functional $J(\mathbf{u}, p, \boldsymbol{\tau}; \mathbf{f})$ over $\boldsymbol{\Phi}$, that is, we seek $(\mathbf{u}, p, \boldsymbol{\tau}) \in \boldsymbol{\Phi}$ such that

$$J(\mathbf{u}, p, \boldsymbol{\tau}; \mathbf{f}) = \inf_{(\mathbf{v}, q, \boldsymbol{\sigma}) \in \boldsymbol{\Phi}} J(\mathbf{v}, q, \boldsymbol{\sigma}; \mathbf{f}). \tag{6}$$

Based on the presentation in [7], we establish the ellipticity of the functional $J(\mathbf{u}, p, \boldsymbol{\tau}; 0)$ in Theorem 1.

Theorem 1. *For $(\mathbf{u}, p, \boldsymbol{\tau}) \in \boldsymbol{\Phi}$, there exist constants c and C, independent of h, such that*

$$c\left(\|\boldsymbol{\tau}\|_0^2 + \|p\|_0^2 + \|\mathbf{u}\|_1^2\right) \le J(\mathbf{u}, p, \boldsymbol{\tau}; 0) \tag{7}$$

and

$$J(\mathbf{u}, p, \boldsymbol{\tau}; 0) \le Ch^{-2}\left(\|\boldsymbol{\tau}\|_0^2 + \|p\|_0^2 + \|\mathbf{u}\|_1^2\right) \tag{8}$$

for any $h < 1$.

Proof. Let $(\mathbf{u}, p, \boldsymbol{\tau}) \in \boldsymbol{\Phi}$. Using the inverse assumption, i.e.,

$$\|\mathbf{u}\|_1 \le Ch^{-1} \|\mathbf{u}\|_0,$$

and the estimate (3) with $q = -1$, we have

$$\|\boldsymbol{\tau}\|_0^2 + \|p\|_0^2 + \|\mathbf{u}\|_1^2 \le C_1 \left(\left\| \boldsymbol{\tau} - \sqrt{2\eta}\mathbf{D}(\mathbf{u}) \right\|_0^2 + \|\nabla \cdot \mathbf{u}\|_0^2 + \left\| -\sqrt{2\eta}\nabla \cdot \boldsymbol{\tau} + \nabla p \right\|_{-1}^2 \right).$$

Since $L^2(\Omega) \subset H^{-1}(\Omega)$, it follows that

$$\begin{aligned}\|\boldsymbol{\tau}\|_0^2 + \|p\|_0^2 + \|\mathbf{u}\|_1^2 &\le C_1\left(\left\|\boldsymbol{\tau} - \sqrt{2\eta}\mathbf{D}(\mathbf{u})\right\|_0^2 + \|\nabla\cdot\mathbf{u}\|_0^2 + \left\|-\sqrt{2\eta}\nabla\cdot\boldsymbol{\tau} + \nabla p\right\|_0^2\right)\\ &\le C_1\left(h^{-2}\left\|\boldsymbol{\tau} - \sqrt{2\eta}\mathbf{D}(\mathbf{u})\right\|_0^2 + h^{-2}\|\nabla\cdot\mathbf{u}\|_0^2 + \left\|-\sqrt{2\eta}\nabla\cdot\boldsymbol{\tau} + \nabla p\right\|_0^2\right)\\ &\le C_1\left(\frac{C_2}{h^2}\left\|\frac{\boldsymbol{\tau} - \sqrt{2\eta}\mathbf{D}(\mathbf{u})}{\sqrt{1+(\dot\gamma)^2}}\right\|_0^2 + \frac{1}{h^2}\|\nabla\cdot\mathbf{u}\|_0^2 + \left\|-\sqrt{2\eta}\nabla\cdot\boldsymbol{\tau} + \nabla p\right\|_0^2\right).\end{aligned}$$

Here the constant $C_2 = 2\max\{1, (\dot\gamma_w)^2\}|\Omega|$, where $\dot\gamma_w$ is the wall shear rate. Hence, (7) is established.

For the upper bound (8), note that

$$\begin{aligned}&\frac{1}{h^2}\left\|\frac{\boldsymbol{\tau} - \sqrt{2\eta}\mathbf{D}(\mathbf{u})}{\sqrt{1+(\dot\gamma)^2}}\right\|_0^2 + \frac{1}{h^2}\|\nabla\cdot\mathbf{u}\|_0^2 + \left\|-\sqrt{2\eta}\nabla\cdot\boldsymbol{\tau} + \nabla p\right\|_0^2\\ &\le \frac{2}{h^2}\left(\|\boldsymbol{\tau}\|_0^2 + \left\|\sqrt{2\eta}\mathbf{D}(\mathbf{u})\right\|_0^2\right) + \frac{1}{h^2}\|\nabla\cdot\mathbf{u}\|_0^2 + \left\|-\sqrt{2\eta}\nabla\cdot\boldsymbol{\tau} + \nabla p\right\|_0^2\\ &\le \frac{2}{h^2}\|\boldsymbol{\tau}\|_0^2 + C_3\|\nabla\cdot\boldsymbol{\tau}\|_0^2 + \frac{C_4}{h^2}\|\mathbf{u}\|_1^2 + \|\nabla p\|_0^2.\end{aligned}$$

Using the inverse inequalities

$$\|\nabla\cdot\boldsymbol{\tau}\|_0 \le Ch^{-1}\|\boldsymbol{\tau}\|_0$$

and

$$\|\nabla p\|_0 \le Ch^{-1}\|p\|_0,$$

we have

$$\begin{aligned}J(\mathbf{u}, p, \boldsymbol{\tau}; 0) &\le 2h^{-2}\|\boldsymbol{\tau}\|_0^2 + C_5h^{-2}\|\boldsymbol{\tau}\|_0^2 + C_4h^{-2}\|\mathbf{u}\|_1^2 + C_6h^{-2}\|p\|_0^2\\ &\le h^{-2}\left((2+C_5)\|\boldsymbol{\tau}\|_0^2 + C_4\|\mathbf{u}\|_1^2 + C_6\|p\|_0^2\right)\\ &\le Ch^{-2}\left(\|\boldsymbol{\tau}\|_0^2 + \|\mathbf{u}\|_1^2 + \|p\|_0^2\right),\end{aligned}$$

where $C = \max\{(2+C_5), C_4, C_6\}$. □

Based on [7,8], we establish error estimates of a discrete nonlinear weighted least-squares finite element approximations in the following. In order to apply the results in [7,8], (5) is replaced with a linearized form. Let $(\mathbf{v}, q, \boldsymbol{\sigma}) = (\tilde{\mathbf{v}}, \tilde q, \tilde{\boldsymbol{\sigma}}) + (\mathbf{v}_0, q_0, \boldsymbol{\sigma}_0)$, where $(\mathbf{v}_0, q_0, \boldsymbol{\sigma}_0)$ is the initial guess and $(\tilde{\mathbf{v}}, \tilde q, \tilde{\boldsymbol{\sigma}})$ is the correction. The nonlinear term in the least-squares functional is then approximated by

$$w_s\left(\boldsymbol{\sigma} - \sqrt{2\eta}\mathbf{D}(\mathbf{v})\right) \approx w_0\left(\left(\tilde{\boldsymbol{\sigma}} - \sqrt{2\eta}\mathbf{D}(\tilde{\mathbf{v}})\right) + \left(\boldsymbol{\sigma}_0 - \sqrt{2\eta}\mathbf{D}(\mathbf{v}_0)\right)\right),$$

where w_0 is computed based on the initial guess $(\mathbf{v}_0, q_0, \boldsymbol{\sigma}_0)$.

Let the initial guess $(\mathbf{u}_0, p_0, \boldsymbol{\tau}_0) \in \boldsymbol{\Phi}^h$. Then the finite element approximation to (6) is equivalent to seek for $(\mathbf{u}^h, p^h, \boldsymbol{\tau}^h) \in \boldsymbol{\Phi}^h$ such that

$$B^h((\mathbf{u}^h, p^h, \boldsymbol{\tau}^h), (\mathbf{v}, q, \boldsymbol{\sigma})) = F^h(\mathbf{v}, q, \boldsymbol{\sigma}), \tag{9}$$

for all $(\mathbf{v}, q, \boldsymbol{\sigma}) \in \boldsymbol{\Phi}^{\mathbf{h}}$, where

$$\begin{aligned}B^h((\mathbf{u}^h, p^h, \boldsymbol{\tau}^h), (\mathbf{v}, q, \boldsymbol{\sigma})) &= h^{-2}\int_\Omega w_0^2\left(\boldsymbol{\tau}^h - \sqrt{2\eta}\mathbf{D}(\mathbf{u}^h)\right) : \left(\boldsymbol{\sigma} - \sqrt{2\eta}\mathbf{D}(\mathbf{v})\right)\mathrm{d}\Omega + Kh^{-2}\int_\Omega\left(\nabla\cdot\mathbf{u}^h\right)(\nabla\cdot\mathbf{v})\,\mathrm{d}\Omega\\ &\quad + \int_\Omega\left(-\sqrt{2\eta}\nabla\cdot\boldsymbol{\tau}^h + \nabla p^h\right)\left(-\sqrt{2\eta}\nabla\cdot\boldsymbol{\sigma} + \nabla q\right)\mathrm{d}\Omega\end{aligned}$$

and

$$\begin{aligned}F^h(\mathbf{v}, q, \boldsymbol{\sigma}) &= h^{-2}\int_\Omega w_0^2\left(\underline{\mathbf{F}}_{\mathbf{1}} - \boldsymbol{\tau}_0 + \sqrt{2\eta}\mathbf{D}(\mathbf{u}_0)\right) : \left(\boldsymbol{\sigma} - \sqrt{2\eta}\mathbf{D}(\mathbf{v})\right)\mathrm{d}\Omega\\ &\quad + Kh^{-2}\int_\Omega(\mathrm{f}_2 - \nabla\cdot\mathbf{u}_0)(\nabla\cdot\mathbf{v})\,\mathrm{d}\Omega + \int_\Omega\left(\mathbf{f}_{\mathbf{3}} + \sqrt{2\eta}\nabla\cdot\boldsymbol{\tau}_0 - \nabla p_0\right)\left(-\sqrt{2\eta}\nabla\cdot\boldsymbol{\sigma} + \nabla q\right)\mathrm{d}\Omega.\end{aligned}$$

Note that (9) can also be obtained by minimizing the functional (5) with $w_s = w_0$ (called J_h). Therefore, using arguments similar to those in [7,8] and Theorem 1, we can establish the unique minimizer of the discrete functional J_h in the following.

Lemma 1. *For any* $(\mathbf{u}, p, \boldsymbol{\tau}) \in \mathbf{H}_0^1(\Omega)^d \times \left(L_0^2(\Omega) \cap H^1(\Omega)\right) \times \left(\underline{\mathbf{L}}^2(\Omega) \cap \mathbf{H}(\mathrm{div}; \Omega)^d\right)$*, there exist constants* c *and* C*, independent of* h*, such that*

$$c\left(\|\boldsymbol{\tau}\|_0^2 + \|p\|_0^2 + \|\mathbf{u}\|_1^2\right) \leq J_h(\mathbf{u}, p, \boldsymbol{\tau}; 0),$$

and

$$J_h(\mathbf{u}, p, \boldsymbol{\tau}; 0) \leq C\left(h^{-2}\|\boldsymbol{\tau}\|_0^2 + \|\nabla \cdot \boldsymbol{\tau}\|_0^2 + h^{-2}\|\mathbf{u}\|_1^2 + \|\nabla p\|_0^2\right). \tag{10}$$

If, in addition, $(\mathbf{u}, p, \boldsymbol{\tau}) \in \boldsymbol{\Phi}^h = \mathbf{V}^h \times Q^h \times \boldsymbol{\Sigma}^h$ *and the spaces* $\boldsymbol{\Sigma}^h$ *and* Q^h *satisfy inverse inequalities*

$$\|\nabla \cdot \boldsymbol{\tau}\|_0 \leq Ch^{-1}\|\boldsymbol{\tau}\|_0$$

and

$$\|\nabla p\|_0 \leq Ch^{-1}\|p\|_0,$$

then (10) *can be replaced by*

$$J_h(\mathbf{u}, p, \boldsymbol{\tau}; 0) \leq Ch^{-2}\left(\|\boldsymbol{\tau}\|_0^2 + \|p\|_0^2 + \|\mathbf{u}\|_1^2\right),$$

for any $h < 1$.

Using Lemma 1 and the Lax–Milgram Lemma, the following theorem is proved.

Theorem 2. *The least-squares functional* (5) *has the unique minimizer out of the space* $\boldsymbol{\Phi}^h$ *for any* $h < 1$.

The following Lemma, which is a special case of the results proved in [7], can be derived based on the solvability of (2).

Lemma 2. *Let* $U = (\mathbf{u}, p, \boldsymbol{\tau}) \in \mathbf{H}_0^1(\Omega)^d \times \left(L_0^2(\Omega) \cap H^1(\Omega)\right) \times \left(\underline{\mathbf{L}}^2(\Omega) \cap \mathbf{H}(\mathrm{div}; \Omega)^d\right)$ *and* $U^h = (\mathbf{u}^h, p^h, \boldsymbol{\tau}^h) \in \boldsymbol{\Phi}^h$ *be as in Lemma 1. Then there exists a constant* C *such that*

$$\left\|\boldsymbol{\tau} - \boldsymbol{\tau}^h\right\|_0 + \left\|p - p^h\right\|_0 + \left\|\mathbf{u} - \mathbf{u}^h\right\|_1 \leq ChB^h(U - U^h, U - U^h)^{\frac{1}{2}}.$$

Using similar arguments in [7] and the approximation properties (4), the following error estimate is established.

Theorem 3. *Let* $U = (\mathbf{u}, p, \boldsymbol{\tau}) \in \boldsymbol{\Phi} \cap \left(\mathbf{H}^{r+2}(\Omega)^d \times \mathbf{H}^{r+1}(\Omega) \times \mathbf{H}^{r+1}(\Omega)^{d\times d}\right)$ *be the solution of the problem* (2) *and* $U^h = (\mathbf{u}^h, p^h, \boldsymbol{\tau}^h) \in \boldsymbol{\Phi}^h$ *denote the solution of the variational problem* (9)*. Then there exists a constant* C *such that*

$$\left\|\boldsymbol{\tau} - \boldsymbol{\tau}^h\right\|_0 + \left\|p - p^h\right\|_0 + \left\|\mathbf{u} - \mathbf{u}^h\right\|_1 \leq Ch^{r+1}\left(\|\boldsymbol{\tau}\|_{r+1} + \|p\|_{r+1} + \|\mathbf{u}\|_{r+2}\right).$$

Note that use of continuous piecewise linear polynomials for all unknowns yields the error estimate

$$\left\|\boldsymbol{\tau} - \boldsymbol{\tau}^h\right\|_0 + \left\|p - p^h\right\|_0 + \left\|\mathbf{u} - \mathbf{u}^h\right\|_1 \leq Ch\left(\|\boldsymbol{\tau}\|_1 + \|p\|_1 + \|\mathbf{u}\|_2\right).$$

It is optimal for the velocity in H^1 norm but suboptimal for pressure p and stress $\boldsymbol{\tau}$. Although the error bounds for the pressure and stress are only $O(h)$ in L^2, optimal rates of convergence are observed in the numerical results presented in Section 3. It appears that the nonlinear weight w_s is essential for optimal convergence when continuous piecewise linear polynomials are used for all unknowns. The importance of w_s in the least-squares approximations is currently under investigation.

3. Numerical results

In this section, two test problems are considered: the flow in the planar channel and the 4 to 1 contraction problem. In our computations, linear basis functions are considered for all variables.

The first problem is the flow in a planar channel on the square domain $[0, 1] \times [0, 1]$ considered in [17]. A uniform directional triangular mesh plotted in Fig. 1 is used for all calculations. The flow domain is shown in Fig. 2. Due to the symmetry along $y = 0$, the computed domain is reduced to half. The velocity $\mathbf{u} = [u, v]^{\mathrm{T}}$ is specified on the inflow, outflow, and wall boundaries. Extra stress $\boldsymbol{\tau}$ is specified on the inflow boundary. Pressure p is set to zero at the point where the outflow boundary meets the wall. On the symmetry boundary, the y-component of $\mathbf{u}$ and τ_{xy} vanish. The exact solutions in Cartesian coordinates are given in [17] by

$$\mathbf{u}_{exact} = \begin{bmatrix} 1 - y^4 \\ 0 \end{bmatrix},$$

and

$$p_{exact} = -x^2.$$

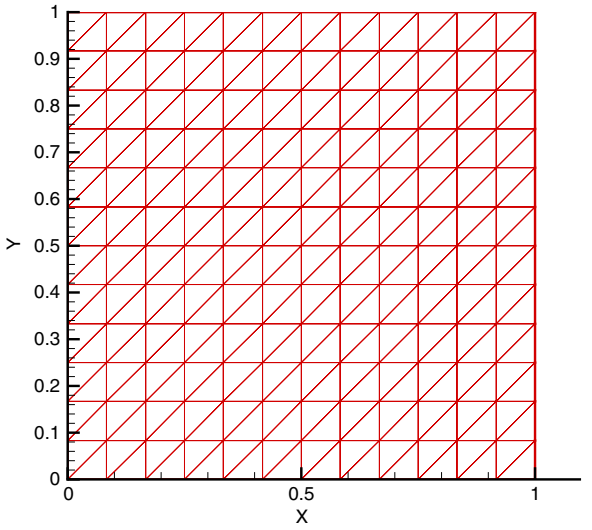

Fig. 1. Triangular mesh corresponding to $h = \frac{1}{16}$.

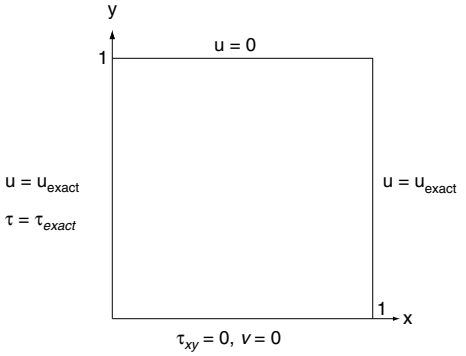

Fig. 2. Test domain with boundary conditions.

Note that the exact solutions are obtained by adding the source term $\mathbf{F}_1 = \mathbf{0}$,

$$\mathbf{f}_3 = \begin{bmatrix} 12y^2 - 2x \\ 0 \end{bmatrix},$$

and the function f_2 is identically zero in (2).

In our computations, the following least-squares functionals for (2) are considered:

1. *The least-squares functional* (LS):

$$J(\mathbf{v}, q, \boldsymbol{\sigma}; \mathbf{f}) = \left\| -\sqrt{2\eta}\nabla \cdot \boldsymbol{\sigma} + \nabla q - \mathbf{f}_3 \right\|_0^2 + \left\| \boldsymbol{\sigma} - \sqrt{2\eta}\mathbf{D}(\mathbf{v}) \right\|_0^2 + \|\nabla \cdot \mathbf{v}\|_0^2 .$$

2. *The weighted least-squares functional* (WDLS):

$$J(\mathbf{v}, q, \boldsymbol{\sigma}; \mathbf{f}) = \left\| -\sqrt{2\eta}\nabla \cdot \boldsymbol{\sigma} + \nabla q - \mathbf{f}_3 \right\|_0^2 + h^{-2} \left\| \boldsymbol{\sigma} - \sqrt{2\eta}\mathbf{D}(\mathbf{v}) \right\|_0^2 + Kh^{-2} \|\nabla \cdot \mathbf{v}\|_0^2 .$$

3. *The nonlinear weighted least-squares functional* (NL-WDLS):

$$J(\mathbf{v}, q, \boldsymbol{\sigma}; \mathbf{f}) = \left\| -\sqrt{2\eta}\nabla \cdot \boldsymbol{\sigma} + \nabla q - \mathbf{f}_3 \right\|_0^2 + h^{-2} \left\| w_s \left(\boldsymbol{\sigma} - \sqrt{2\eta}\mathbf{D}(\mathbf{v}) \right) \right\|_0^2 + Kh^{-2} \|\nabla \cdot \mathbf{v}\|_0^2 ,$$

where the nonlinear weights w_s is defined in (6).

The coefficient $K = 1$ related to the mass conservation is considered first in the WDLS and NL-WDLS functionals. The L^2 errors of various least-squares solutions for Stokes equations are shown in Fig. 3. From Fig. 3, observe that the improvement

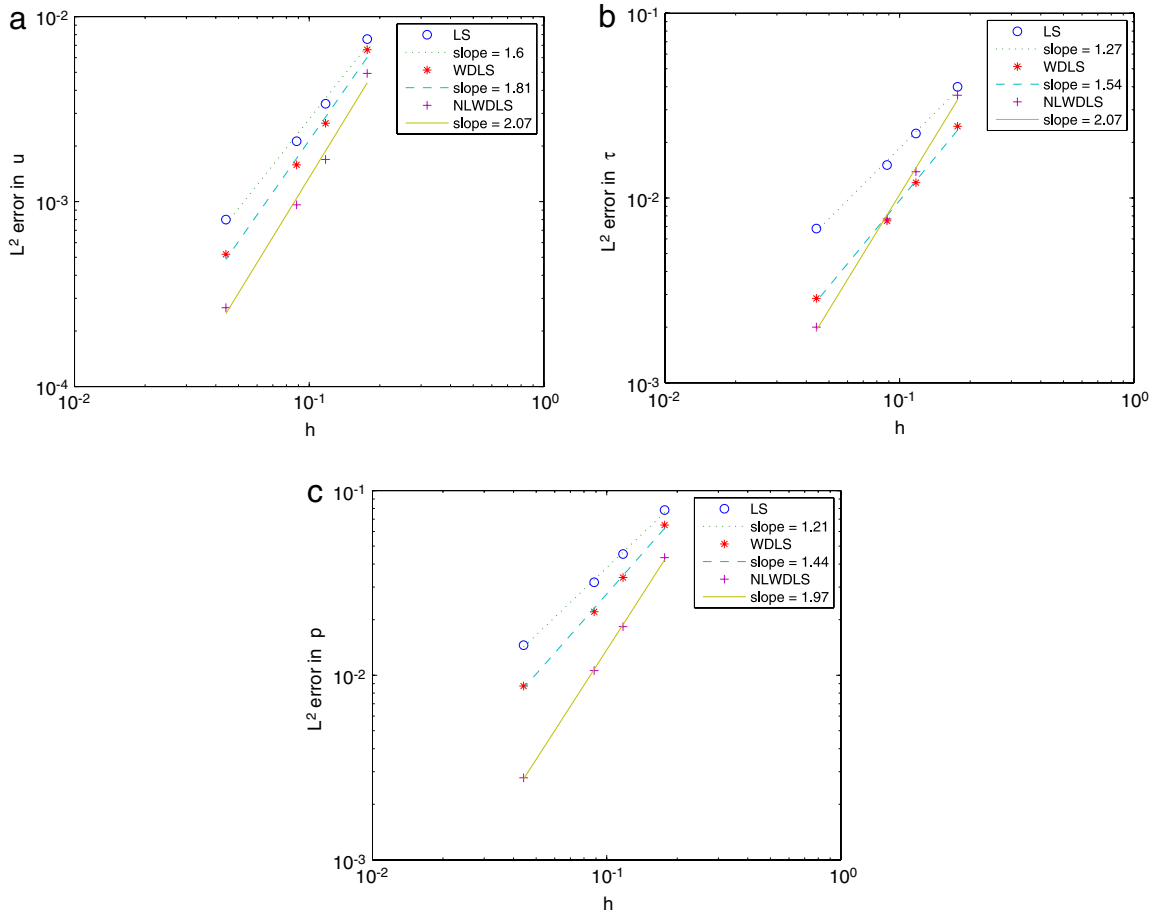

Fig. 3. $K = 1$ for WDLS and NL-WDLS. L^2 errors in (a) $\mathbf{u}$, (b) $\boldsymbol{\tau}$ and (c) p of LS (o), WDLS (*) and NL-WDLS (+) solutions.

of the rate of convergence of the WDLS over LS. This is consistent with results obtained for the Stokes equations, [7]. Note also that the rate of convergence of the NL-WDLS improves over the WDLS. In fact, optimal convergence of the NL-WDLS are obtained in $\mathbf{u}$, $\boldsymbol{\tau}$ and almost optimal convergence are obtained in p. Based on these results, the rate of convergence can be restored with careful selections of nonlinear weighting functions w_s. In addition, the results suggest that the w_s considered in our computations is optimal.

To investigate the influence of the mass conservation, in Fig. 4, we report results of various weights $K = 1, 10, 10^2, 10^6$ and 10^8 in the nonlinear weighted least-squares (NL-WDLS) functionals. Observe that optimal rates of convergence in L^2-norm for $\mathbf{u}$, p and $\boldsymbol{\tau}$ are obtained by increasing K. These results indicate that the solutions can be improved by increasing the importance of the mass conservation equation relative to the remaining ones. In addition, Fig. 4 shows that results of the cases when $K = 10^2, 10^6$, and 10^8 are almost identical. Based on our experience, convergent rates for the NL-WDLS solutions with $K = 10^2$ agree well with those of $K > 10^2$. Therefore, it is sufficient to choose $K = 10^2$ for satisfactory results.

To illustrate further the capability of the NL-WDLS schemes, the following benchmark problem has been chosen: the Stokes flow pass through a 4 to 1 contraction channel. The computational domain and the boundary conditions are described in Fig. 5. Due to the symmetry along $y = 0$, the computation domain is reduced to half. The ratio of the height of downstream and upstream channels is set to 4. The boundary conditions are taken from those given in [12]. On the symmetry boundary, the y-component of $\mathbf{u}$ and τ_{xy} vanish. Pressure p is set to zero on the outlet of the domain. On the wall, all components of $\mathbf{u}$ are zero. In our computations, $-2 \le x \le 5$ is used which corresponds to the upstream length $X_u = 8L$ and the downstream length $X_d = 20L$, where L is the downstream channel half-width. In [12], $-20L \le x \le 50L$ is considered and a transient finite element method is used to obtain high-resolution solutions for viscoelastic 4 to 1 planar contraction flow problems using a minimum spacing of 0.0056. Although our domain $-8L \le x \le 20L$ is much smaller than the domain used in [12], the flow is fully developed in this region. Therefore, our results can be compared to those obtained in [12].

In our computations, as illustrated in Fig. 6, the Union Jack grid with the uniform mesh spacing of 0.0179 on $[-2, 2]$ and 0.025 on $[2, 5]$ is considered. In [10], such grid is illustrated to have special properties not necessary possessed by other configurations. The computational results are presented based on the velocity component along the axis of symmetry and corner vortex behaviors.

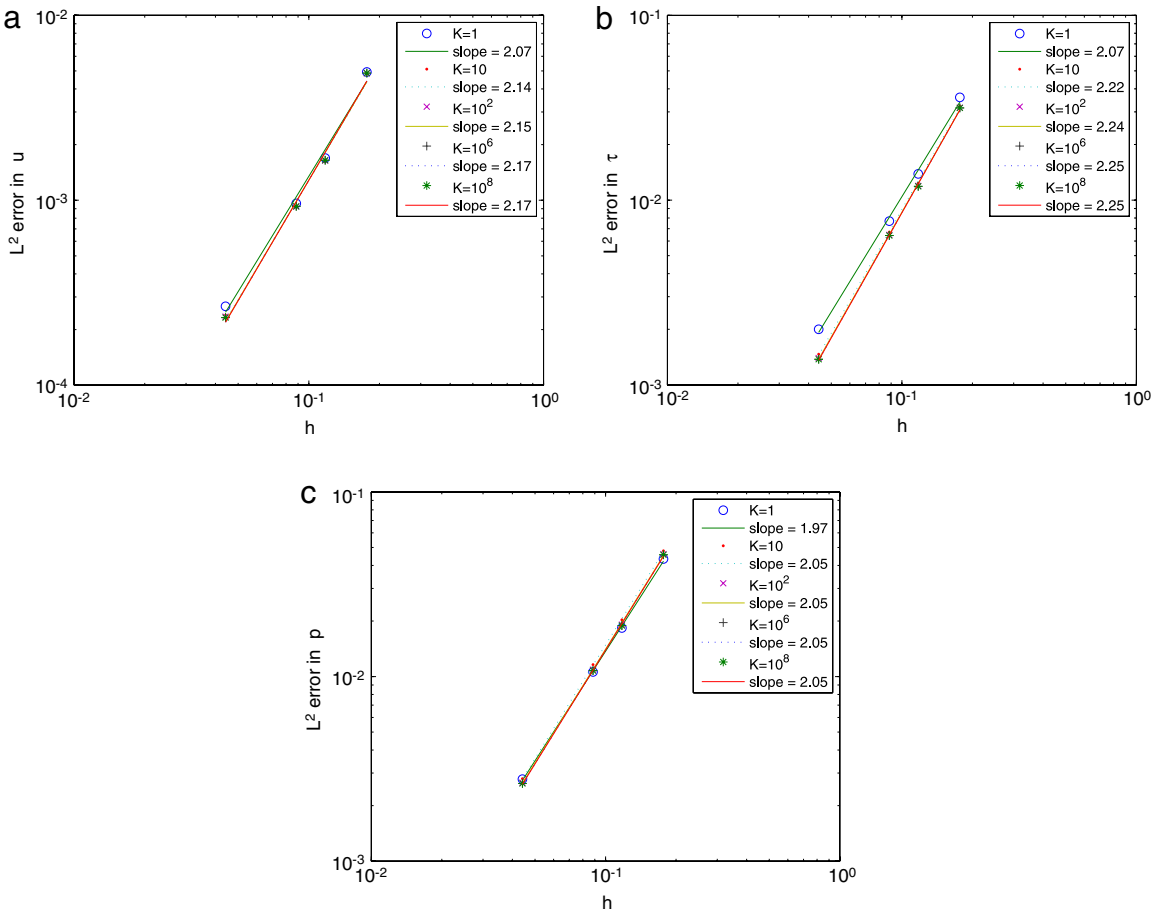

Fig. 4. L^2 errors in (a) $\mathbf{u}$, (b) $\boldsymbol{\tau}$ and (c) p of NL-WDLS solutions using $K = 1$ (o), $K = 10$ (.), $K = 10^2$ (x), $K = 10^6$ (+) and $K = 10^8$ (*).

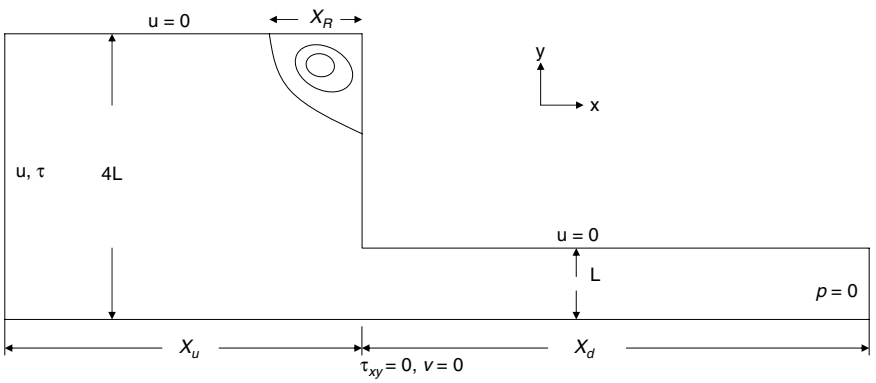

Fig. 5. The 4 to 1 contraction domain with boundary conditions.

The WDLS and NL-WDLS functionals are both considered for this 4 to 1 contraction problem. Recall that for the flow in a planar channel, it is necessary to choose the proper weight K in these functionals for optimal results. Using weights ranging from $K = 10^2$ to 10^8 in the WDLS and NL-WDLS functionals, the solutions u along the axis of symmetry are plotted in Figs. 7 and 8, respectively. The results indicate that when $K > 10^5$, u along the axis of symmetry for the WDLS and NL-WDLS solutions are similar and agree well with those of $K = 10^5$. It is thus sufficient to choose $K = 10^5$ for satisfactory results. In addition, as illustrated from Figs. 7 and 8, u along $y = 0$ on the outlet using the WDLS and NL-WDLS methods are over 0.375 and approximately 0.375, respectively. In Fig. 9, the streamline patterns of the WDLS and NL-WDLS formulations using $K = 10^5$ are plotted. Observe that the sizes of the corner vortex X_R using the WDLS and NL-WDLS are approximately 0.54 and 0.37,

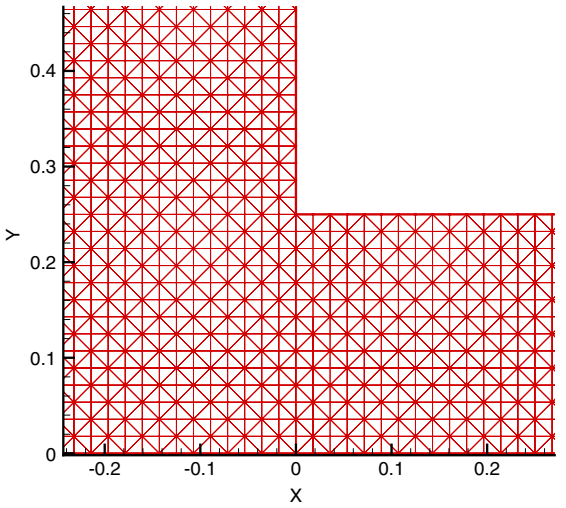

Fig. 6. Union Jack grid with a minimum mesh length of 0.0179 near the singularity.

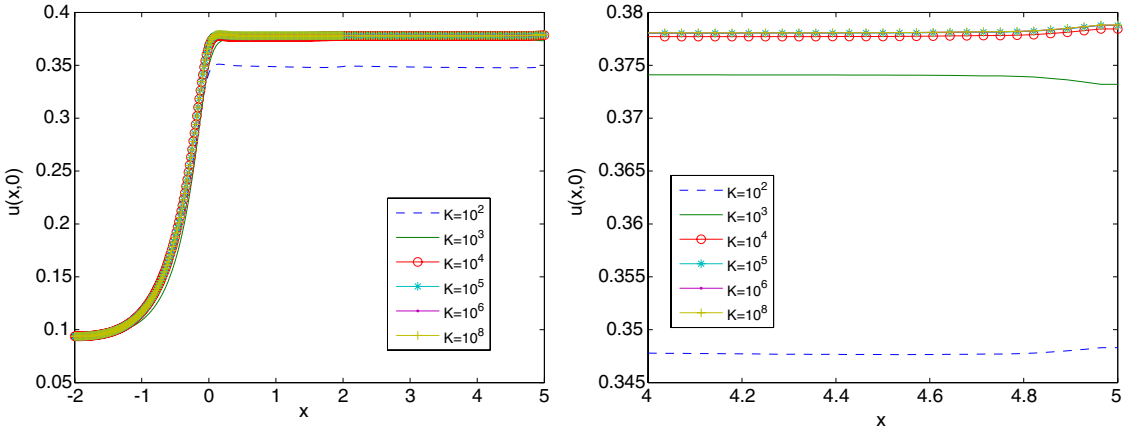

Fig. 7. WDLS method. Plots of **u** (left) along the axis of symmetry using $K = 10^2$ (- -), $K = 10^3$ (–), $K = 10^4$ (o), $K = 10^5$ (*), $K = 10^6$ (.) and $K = 10^8$ (+) and near the outlet (right).

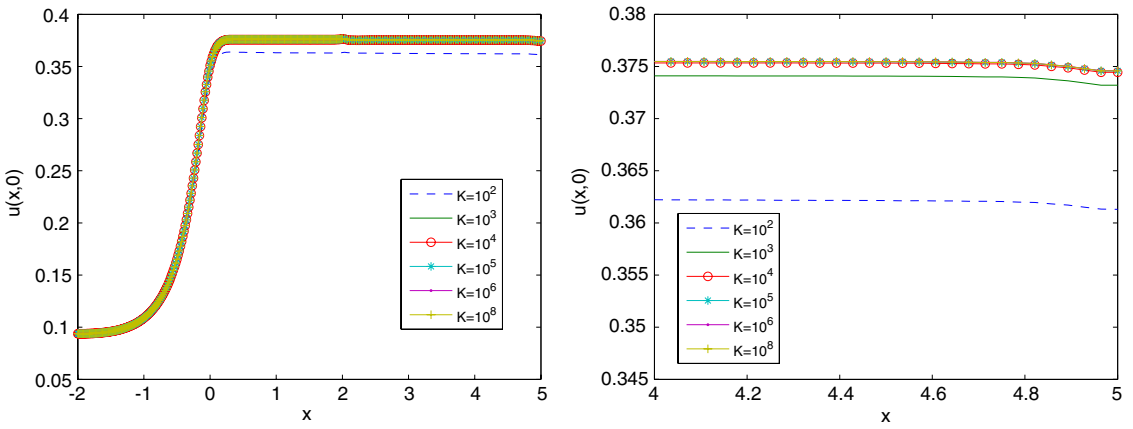

Fig. 8. NL-WDLS method. Plots of **u** (left) along the axis of symmetry using $K = 10^2$ (- -), $K = 10^3$ (–), $K = 10^4$ (o), $K = 10^5$ (*), $K = 10^6$ (.) and $K = 10^8$ (+) and near the outlet (right).

respectively. Note that in [12], u along $y = 0$ on the outlet is approximately 0.375 and X_R is approximately 0.375. Therefore, the NL-WDLS method outperforms the WDLS method and gives results which are compatible to those presented in [12].

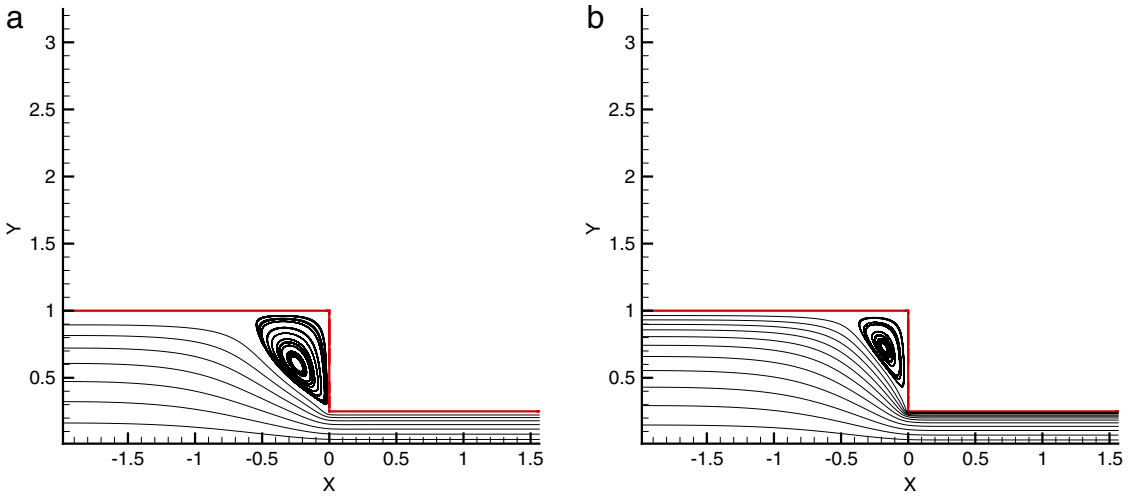

Fig. 9. Streamlines in **u** of (a) WDLS and (b)NL-WDLS methods.

4. Conclusions

We have presented a nonlinear weighted least-squares finite element approximation to Stokes problems. Comparisons are made with least-squares formulations with no weights and with a simpler mesh dependent weighting scheme. Based on the above, there is a significant difference between the results among the least-squares approaches, confirming that using linear polynomials in all variables, we are able to obtain optimal convergence in all variables in the NL-WDLS methods. This resolves one of the difficulties associated with low order basis functions used in least-squares method for Stokes equations, [7,8]. In addition, we have illustrated the importance of the mass conservation equation in the least-squares functionals. In particular, using $K = 10^5$, the solutions can be improved greatly to achieve accurate results in the 4 to 1 contraction problem. These results suggest that the mass conservation constant varies with the problems. Furthermore, numerical experiments indicate that the method can be extended to more general 4 to 1 contraction problems without major difficulty. Finally, the error estimates in Section 2 do not reflect the optimal convergence obtained in the NL-WDLS methods when linear polynomials are used in all variables. These issues will be investigated further in the future.

Acknowledgements

The first author was supported in part by Wenzao Ursuline College of Languages of Taiwan. The second author was supported in part by the National Science Council of Taiwan under contract number 96-2115-M-194-008.

References

[1] P.B. Bochev, M.D. Gunzburger, Finite element methods of least-squares type, SIAM, Review 40 (1998) 789–837.
[2] A. Bose, G.F. Carey, Least-squares p-r finite element methods for incompressible non-Newtonian flows, Comput. Methods Appl. Mech. Engrg. 180 (1999) 431–458.
[3] Z. Cai, T.A. Manteufeel, S.F. Mccormick, First-order system least-squares for velocity-vorticity-pressure form of the Stokes equations, with application to linear elastically, Eectronic Transactions on Numerical Analysis 3 (1995) 150–159.
[4] G.F. Carey, A.I. Pehlivanov, Y. Shen, A. Bose, K.C. Wang, Least-squares finite elements for fluid flow and transport, Int. J. Numer. Methods Fluids 27 (1998) 97–107.
[5] B.N. Jiang, C.L. Chang, A Least-squares finite elements for the Stokes problem, Comput. Methods Appl. Mech. Engrg. 78 (1990) 297–311.
[6] H.C. Lee, Adaptive least-squares finite elements methods for viscoelastic flow problems, Ph.D. Thesis, Dept. of Mathematics, National Chung Cheng University, Taiwan, 2008.
[7] P.B. Bochev, M.D. Gunzburger, Least-squares for the velocity–pressure–stress formulation of the Stokes equations, Comput. Methods Appl. Mech. Engrg. 126 (1995) 267–287.
[8] S.D. Kim, B.C. Shin, H^{-1} least-squares method for the velocity–pressure–stress formulation of Stokes equation, Appl. Numer. Math. 40 (2002) 451–465.
[9] C.L. Chang, J. Nelson, Least-squares finite element method for the Stokes problem with zero residual of mass conservation, SIAM J. Numer. Anal. 34 (1997) 480–489.
[10] P. Bolton, R.W. Thatcher, On mass conservation in least-squares methods, J. Comput. Phys. 203 (2005) 287–304.
[11] V. Prabhakar, J.P. Pontaza, J.N. Reddy, A collocation penalty least-squares finite element formulation for incompressible flows, Comput. Methods Appl. Mech. Engrg. 197 (2008) 449–463.
[12] J.M. Kim, C. Kim, J.H. Kim, C. Chunga, K.H. Ahna, S.J. Lee, High-resolution finite element simulation of 4:1 planar contraction flow of viscoelastic fluid, J. Non-Newtonian Fluid Mech. 129 (2005) 23–37.
[13] J.M. Deang, M.D. Gunzburger, Issues related to least-squares finite element methods for the Stoke equations, SIAM J. SCI. Comput. 20 (3) (1998) 878–906.
[14] T.F. Chen, Weighted least-squares approximations for nonlinear hyperbolic equations, Comput. Math. Appl. 48 (2004) 1059–1076.
[15] T.F. Chen, C.L. Cox, H.C. Lee, K.L. Tung, Least-squares finite elements for generalized Newtonian and viscoelastic flows, Applied Numerical Mathematics, 2009 (submitted for publication).
[16] Y. Son, Determination of shear viscosity and shear rate from pressure drop and flow rate relationship in a rectangular channel, Polymer 48 (2007) 632–637.
[17] A. Fortin, R. Guenette, R. Pierre, On the discrete EVSS method, Comput. Methods Appl. Mech. Engrg. 189 (2000) 21–139.